17th International Conference on Pattern Recognition
Cambridge, United Kingdom, 23-26 August 2004

Automated Detection of Solar Loops by the Oriented Connectivity Method

Jong K. Lee (UAH), Timothy S. Newman(UAH), and G. Allen Gary (MSFC)

Abstract

An automated technique to segment solar coronal loops from intensity images of the Sun's corona is introduced. It exploits physical characteristics of the solar magnetic field to enable robust extraction from noisy images. The technique is a constructive curve detection approach, constrained by collections of estimates of the magnetic field's orientation. Its effectiveness is evaluated through experiments on synthetic and real coronal images.

1. Introduction

The Sun is a dynamic force that greatly impacts the solar system. In particular, solar activity can impact terrestrial communication and weather. Solar physicists are currently attempting to gain a stronger understanding of solar dynamism, partially via study of solar magnetism.

One key means to study solar dynamism is by observation and analysis of the solar magnetic field from solar satellite images. In particular, solar physicists are interested in examining images of the solar corona. NASA's ongoing TRACE satellite mission, which collects high-resolution (512×512) intensity images of the Sun's corona several times per hour, is a preferred source of such images. (A sample TRACE image is shown in Fig. 1(a).) The primary examination task is to detect and identify the solar coronal loop structures in these images. Previously, automatic means to detect and identify such structures haven't been successful; current scientific study of solar coronal loops requires manual extraction of the loop structures from images. Detection of coronal loops is challenging, even using TRACE images, because the loop structures tend to have blurry boundaries and overlap in the imagery. Many loops also have low contrast sub-segments. (The intensity of such sub-segments is relatively lower than that of other sub-segments.) In addition, there is impulse noise in the images.

In this paper, a new technique, the Oriented Connectivity Method, for automated segmentation of coronal loops from images of the Sun's corona is introduced. The technique exploits constraints based on physical properties to guide the curve detection process.

2. Related Work

A number of methods for representing, following, and linking edge structures in intensity images have been presented in the literature. For example, since the early 60's, starting with Freeman's [2] well-known chain coding, a number of structure boundary representation mechanisms have been presented. Many edge linkage approaches have also been described. For example, Makhervaks *et al*. [7] have recently presented an edge linkage process that joins edge structures using an edge-explorer operator that acts on a gradient vector field.

Curve feature detection techniques have also been described. For instance, Canning *et al*. [1] have detected thin curve features by examining pixel neighborhoods to identify local gray level patterns that are consistent with the presence of an edge. Adjacent, compatible edge pixels are then linked. Jang and Hong [4] have detected curvilinear structures (e.g., a line or a curve of a given width) using skeleton extraction. They use Canny edge detection to define the boundary points of the regions in which the skeleton extraction will be performed.

Hough-based techniques [3] have also been utilized in curve detection. Their large parameter space for large images and for complex shapes, such as in our problem domain, is a difficulty, however. Active contour models (i.e., snakes [5]), which are typically defined as energy-minimizing splines, have also been widely used for detecting curved structure boundaries. A difficulty with using snakes for coronal loop detection is that there are many nearby loops and the loops cross each other, so it is easy for a single snake to lock onto components of multiple loops. Coronal loop crossings also complicate use of many other curve detection schemes.

Strous [9] has described a pixel labeling algorithm for coronal images. The algorithm labels a pixel as a member of a loop structure if the pixel's intensity is higher than those of more than two of the four cross-pairs in its 3×3 neighborhood (and as a non-member otherwise). Since the pixels on the central axis of the coronal loop structures are usually brighter than the neighboring pixels, Strous's algorithm detects most of the coronal loop *pixels*. It does not detect *loops* per se, however, as it has no process to link pixels into loop structures. In addition, the algorithm falsely labels as loop pixels many noisy background pixels and many bright pixels not actually on coronal loops.

3. Coronal Loop Detection Methodology

Next, we describe our new Oriented Connectivity Method (OCM), which is based partly on Strous's loop pixel labeling [9]. The Oriented Connectivity Method constructively segments the coronal loops while simultaneously eliminating false loop pixels. The approach's processing includes steps that achieve joining of disconnected loop sub-segments, thus forming descriptions of complete loops. The Oriented Connectivity performs its loop segmentation by exploiting a physical constraint, namely the local orientation of the solar magnetic field. Since coronal loops align with the solar magnetic field, we exploit knowledge of the field to aid the linkage process.

Magnetic fields, including local fields in regions about the Sun, can be reasonably approximated in 3D space by a dipole field model [6]. One complication in using this 3D spatial model to guide loop detection in the coronal intensity images is that the intensity images record the projection of 3D structures onto 2D image space. The Sun's field is also a collection of many dipoles, and the position of each needs to be estimated. Thus, many points in 3D space, each with a different local magnetic field orientation, could project to each pixel. The 3D-to-2D-projected loops could also cross each other.

In our approach, we exploit the dipole field model by, at each pixel labeled as a loop pixel after application of Strous's algorithm, considering a set of estimates of the 3D-to-2D-projected magnetic fields' orientations. We use these estimates to progressively link pixels with consistent magnetic field orientation. The set of estimates are taken from a set of azimuth maps (of the magnetic field) from a solar magnetogram. Each azimuth map records an estimate of the angular direction of the magnetic field and is defined for one height above the solar surface, so for small regions of the solar surface each azimuth map is a map of the magnetic field's orientations at a given height (i.e., in z). The azimuth can be derived from the vector sum of the x and y components (i.e., B_x and B_y) of the magnetic dipole flux density equation [8]:

$$B_x = B_o \frac{3xz}{r^5}, \quad B_y = B_o \frac{3yz}{r^5}, \qquad (1)$$

where x, y, and z are the Cartesian components of the magnetic field position vector, r is the magnitude of the position vector, and B_o is the magnetic force constant.

3.1. Preprocessing

The Strous's algorithm [9] (that our approach is based upon) produces a poor labeling when applied to a raw TRACE image, partially due to the known imaging effects described earlier. Thus, to remove impulse noise and to improve the contrast between the loops and the background, prior to applying the Strous algorithm, we have applied median filtering followed by unsharp masking as preprocessing steps. We empirically determined that 7×7 median filtering could eliminate much of the impulse noise. The unsharp masking used a blurred image obtained from 11×11 linear smoothing.

Fig. 1(a) shows a sample coronal image. The result from median filtering that image is shown in Fig. 1(b). The contrast-enhanced result of the unsharp masking on the same underlying image is shown in Fig. 1(c). As shown in these figures, the impulse noises are removed and the loop structures are sharpened by the preprocessing.

The Strous's loop pixel labeling [9], even when applied to an image "cleaned" by median filtering and unsharp masking, still wrongly classifies many noise pixels and bright pixels that are not on the coronal loop structures. The low contrast and the blurriness of the coronal loop structures are largely responsible for these falsely-labeled pixels. We have found that these falsely-labeled pixels can be largely removed by a combination of global and adaptive thresholdings applied to the image "cleaned" by median filtering and unsharp masking.

We first apply a global thresholding. Its threshold is the median intensity T of the filtered images; all pixels whose intensity is less than T are considered to be non-loop pixels. Next, additional falsely-labeled pixels are removed by an adaptive thresholding step. The adaptive thresholding performs thresholding in each sub-region of the image. We have found empirically that dividing the image into 31×31 pixel tiles with 50% overlap (e.g., the top-half of a sub-region R_B overlaps the bottom-half of a region R_A that is above sub-region R_B) produces reasonable results. The threshold used in each sub-region is the sub-region's median intensity value. In fact, wherever sub-regions overlap, the threshold for the overlapped area is the mean of the thresholds of the overlapping sub-regions. Fig. 1(d) shows the result after applying the two thresholdings to a "cleaned" image (i.e., of Fig. 1(c)). Many, but not all, falsely-labeled pixels in this figure have been removed by the thresholdings.

3.2. Oriented Connectivity Method

Our Oriented Connectivity Method's constructive curve detection starts from any pixel labeled as a coronal loop pixel and then forms a clustering of all the other pixels that define the same loop structure. This process is applied repeatedly until all pixels labeled as loop pixels have been processed. Although any scanning process can be used to find the starting points on each loop, we have found that a process that searches for a starting point in a column-wise process followed by a row-wise process is

typically sufficient to find the major loop structures. (We've also found it's sufficient to perform the column- (row-) wise search only every twentieth column (row).)

The forming of a clustering of pixels into a loop is a stepwise process which at each step adds one pixel to the current loop. The "best" pixel to be added is found by a search from the current loop's end pixel. A small fan-shaped region (the "searching region") about that pixel is where the search occurs. The searching region's fan shape is bounded by the magnetic field minimum and maximum angular directions (azimuths) for that pixel. The region's extent d was empirically determined to be 5 pixels. An example of the searching region for a pixel S is shown in Fig. 3. In the figure, the arrows represent the azimuths at different heights. The thick arrows represent the extremal azimuths. The "best" pixel in the region is the one that best-preserves loop continuity in position and tangent direction and which is nearby and sufficiently bright. We have encoded the degree of goodness of each candidate pixel using a weighting scheme based on distance, intensity, angular, and tangent weighting factors. The highest weighted pixel is the one joined to the current loop. The constructive process is repeated until no other pixels can be joined to a loop segment end point. The steps of the Oriented Connectivity Method algorithm are as follows.

Step 1. Apply Strous's loop pixel labeling (to a "cleaned" image).

Step 2. Start forming a (new) loop from an unassigned pixel P_i that's labeled as a loop pixel.

Step 3. Define the searching region at P_i.

Step 4. Find the unassigned loop-labeled pixels in the searching region of P_i.

Step 5. If there are no loop-labeled pixels in the searching region, find a loop-labeled pixel in the 8-neighborhood of P_i. If one exists, apply Step 7.

Step 6. If there is no loop-labeled pixel in the neighborhood, repeat Step 2. If so, set the loop-labeled neighborhood pixel as a new starting point and repeat Step 3.

Step 7. Apply weighting scheme to find each pixel's goodness.

Step 8. Assign the highest-weighted pixel in the searching region as the next pixel, P_{i+1}, of the loop.

Step 9. Connect P_i and P_{i+1}, save P_{i+1} as new P_i.

Step 10. Repeat Steps 2 to 8 until no other points are selected.

Step 11. Calculate the mean width of the detected loop.

Step 12. Remove the detected loop from the image and save its description.

Step 13. Repeat Steps 1 to 11 until all image pixels have been considered.

In Step 11, mean width is determined from the intensity profiles at three points (the midpoint and points halfway between the midpoint and endpoints) of the detected loop. At each point, loop width is defined to be the distance (measured perpendicularly to the loop's local direction) between the maximum gradient points on each side of the loop.

3.3. Post-processing

The Oriented Connectivity Method can miss some loops and over-segment (i.e., disconnect) others. The pixel-by-pixel linking process may also produce aliased (i.e., jaggy) loop structures. To remove the aliasing and join the disconnected sub-segments of the loops, we post-process the OCM's output by applying B-spline fitting and edge linking. The first B-spline fitting is designed to produce smooth loop curves. In our usage of B-spline fitting, different number of equally-spaced loop points are used for the control points according to the length of each loop to be fit (i.e., more control points are used to represent a longer loop). Then a simple edge linking and the second B-spline fitting are applied to the result of the first B-spline fitting to merge disconnected loop segments smoothly: namely, if two loop segments terminate a short distance from each other, they are linked provided that they have similar tangent directions at their end points.

4. Experimental Results

We have evaluated the effectiveness of the Oriented Connectivity Method (OCM) using synthetic and real coronal images.

To benchmark the OCM's effectiveness, we applied (1) a manual method (which we will label MM) that involved manually identifying as many coronal loop points as possible, and (2) a semi-manual method (which we will label SMM) that involved manually sampling several coronal loop points and using the points sampled on each loop as the control points of a B-spline fitting. These two manual methods and the OCM were applied on synthetic datasets of size 500×500 which were created by projecting a collection of 3D field lines generated from three known dipoles onto a 2D image.

The benchmarking considered the global positional error (GPE) and four metrics on this error (e.g., the maximum, the minimum, the mean, and the standard deviation of the positional error). This error measures the distance of traced/detected curves from the known loop centers. The GPE is measured over all loops. Fig. 2(a) shows a synthetic dataset and the blue curves in Fig. 2(b) represent the loops detected in this image by the OCM. As shown in Fig. 2(b), our technique detected most of the loops that are easily visible to human vision. The global error measures for the two manual methods and the OCM

on the synthetic image shown in Fig. 2 are listed in Table 1. The Oriented Connectivity Method produced smaller errors and had less variance in position on its loops. However, the number of traced/detected loops were 74, 69, and 57 for the MM, SMM, and OCM, respectively.

We have also applied the Oriented Connectivity Method to seven real coronal images. To analyze the effectiveness of the Oriented Connectivity Method, eight coronal loops were selected arbitrarily on each image and then the images were considered by the semi-manual method and by the OCM. Three classes of error were measured: the number of false positives, errors in length, and the positional errors. There were 4 global false positive errors (i.e., four loop structures were detected by the semi-manual method but not detected by the Oriented Connectivity Method) in the collection of tests. The OCM tended to over-segment loops; the average loop lengths from OCM were 44% shorter than the loop lengths from SMM. The average relative global position error for the Oriented Connectivity Method was 3.30 pixels. The result for the image shown in Fig. 1(a) is shown in Fig. 1(e). The blue curves in Fig. 1(e) represent the loops detected by the Oriented Connectivity Method; the technique reasonably detected the well-defined loops.

5. Conclusions

We have presented a new method of detecting solar coronal loop structures. The Oriented Connectivity Method, the first automated coronal loop detection technique, uses physical constraints to guide the coronal curve detection process. Through evaluation of the technique we have shown that the technique can provide consistent and reasonable automated detections of loop structures in solar coronal images.

For the future work, additional image processing techniques to sharpen the coronal loops and other techniques to more strongly exploit the orientation of the magnetic field will be explored.

Similarly-shaped structures in other scientifically-interesting environments are influenced by other characterizable physical properties, thus extending the Oriented Connectivity Method to other arenas may be possible.

References

[1] J. Canning, J. J. Kim, N. Netanyahu, and A. Rosenfeld, "Symbolic Pixel Labeling for Curvilinear Feature Detection," *Pattern Recog. Letters*, Vol. 8 (5), Dec. 1988, pp. 299-310.

[2] H. Freeman, "On the Encoding of Arbitrary Geometric Configurations," *IRE Trans. on Electronic Computers*, Vol. 10, 1961, pp. 260-268.

[3] P.V.C. Hough, "Method and Means for Recognizing Complex Patterns," *U.S. Patent*, *3,069,654*, Dec. 1962.

[4] J. Jang and K. Hong, "Detection of Curvilinear structures and Recognition of Their Regions in Gray-scale Images," *Pattern Recog.*, Vol. 35 (4), Apr. 2002, pp. 807-824.

[5] M. Kass, A Within, and D. Terzopoulos, "Snakes: Active Contour Models," in *Proc. of 1st Int'l Conf. on Computer Vision*, London, 1987, pp 259-269.

[6] T. Magara and D.W. Longcope, "3-Dimensional Evolution of a Magnetic Flux Tube Emerging into the Solar Atmosphere," *EOS Trans. American Geophysical Union*, 2002, pp. A441.

[7] V. Makhervaks, G. Barequet, and A. Bruckstein, "Image Flows and One-liner Graphical Image Representation," in *Proc. of the 16th Int'l Conf. on Pattern Recog.,* Quebec City, Aug. 2002, Vol. 1, pp. 640-643.

[8] R. Plonesy and R.E. Collin, *Principles and Application of Electromagnetic Fields*, McGraw Hill, New York, 1961.

[9] L.H. Strous, "Loop Detection," http://www.lmsal.com/~aschwanden/stereo/2000easton/cdaw.html, accessed on Oct. 12, 2002.

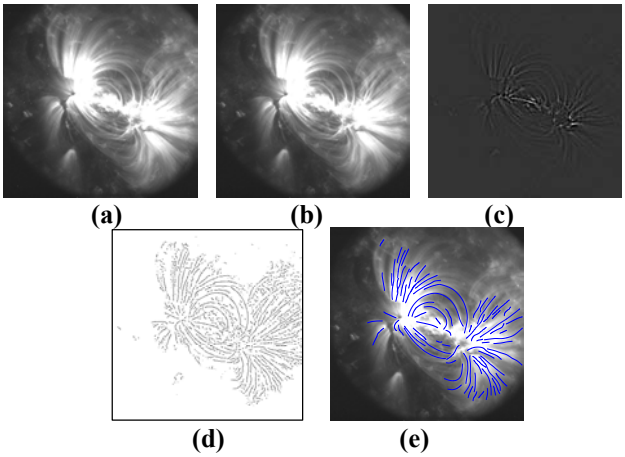

Fig. 1. (a) Coronal image, (b) Median filtered image, (c) Contrast enhanced version of unsharp masked image, (d) Curve features after thresholdings (e) Detected loops.

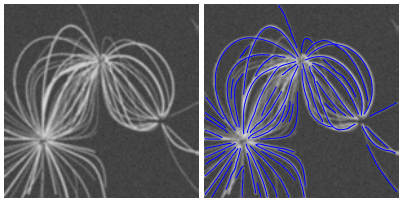

Fig. 2. (a) Synthetic image, (b) Detected loops

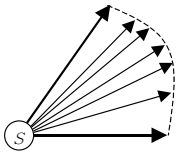

Fig. 3. Search Region about S

Table 1. Errors (GPE) on synthetic image (in pixels)

Method	Max	Min	Mean	Std Dev
MM	3.61	0.00	0.66	0.63
SMM	3.51	0.00	0.58	0.40
OCM	3.00	0.00	0.57	0.37